Molecular dynamics of the liquid-gas phase transition

Mark Gorenstein

Bogolyubov Institute for Theoretical Physics, 03680 Kyiv, Ukraine

November 25, 2025

Phase transition(s) in strongly interacting matter

Liquid-gas first order phase transitions

1. Nuclear Matter

$$\text{Experimental estimates}: \quad T_c \cong 15 \text{ MeV} \ , \quad n_c \cong 0.07 \text{ fm}^{-3} \tag{1}$$

2. QCD FOPT at finite baryon density

$$T_c = ? \ , \quad n_B = ? \tag{2}$$

Plan

1. Introduction (van der Waals model)
2. Molecular Dynamics with Lennard-Jones Potential
3. Liquid-gas phase transition and critical point
4. Particle number fluctuations
5. Summary

Volodymyr Kuznietsov, Oleh Savchuk, Roman Poberezhnyuk, Volodymyr Vovchenko, Mark Gorenstein, Volker Koch, and Horst Stoecker
Phys. Rev. C 104 (2021) 5, 055202
Phys. Rev. C 105 (2022) 4, 044903
Phys. Rev. C 107 (2023) 5, 055206
Phys. Rev. C 110 (2024) 1, 015206

arXiv:2511.00755 (**EMMI, GSI November 2025**)

Connection to the experiment

Theory

- Contact with the heat bath
- GCE conservation of charges
- Uniform system
- Fixed volume
- Coordinate space

Experiment

- Expanding in vacuum
- Global charge conservation
- Inhomogenous
- Fluctuating
- Momentum space

Need microscopic description of fluctuations

Famous example of EoS with LGPT and critical point

van der Waals: 1873 (PhD), 1910 (Nobel Prize)

$$p = \frac{TN}{V - bN} - a\,\frac{N^2}{V^2} = \frac{Tn}{1 - bn} - an^2 \tag{3}$$

$$\left(\frac{\partial p}{\partial n}\right)_T = 0\,, \quad \left(\frac{\partial^2 p}{\partial n^2}\right)_T = 0\,. \tag{4}$$

$$T_\mathrm{c} = \frac{8a}{27b}\,, \quad n_\mathrm{c} = \frac{1}{3b}\,, \quad p_\mathrm{c} = \frac{a}{27b^2}\,. \tag{5}$$

1. CE $\rightarrow$ GCE
2. Fermi statistics of nucleons.
3. Ground state: $T = 0\,, \quad n_0 = 0.16~\mathrm{fm}^{-3}, \quad W_o = -16~\mathrm{MeV} \rightarrow a, b$

Vovchenko, Anchishkin, Gorenstein, Phys. Rev. C (2015)

$T-\mu$ Phase diagram

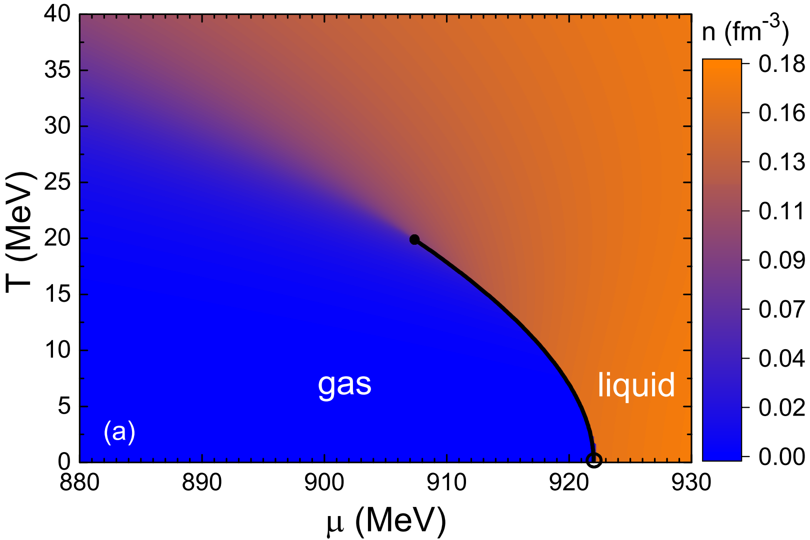

Particle number fluctuations

$$\sigma^2 \equiv \langle (\Delta N)^2 \rangle \ , \qquad \Delta N \equiv N - \langle N \rangle \ , \tag{6}$$

$$\omega[N] \ = \ \frac{\sigma^2}{\langle N \rangle} \quad \text{scaled variance} \ , \tag{7}$$

$$S\sigma \ = \ \frac{\langle (\Delta N)^3 \rangle}{\sigma^2} \quad \text{skewness} \ , \tag{8}$$

$$\kappa\sigma^2 \ = \ \frac{\langle (\Delta N)^4 \rangle - 3\langle (\Delta N)^2 \rangle^2}{\sigma^2} \quad \text{kurtosis} \ . \tag{9}$$

$$\kappa_n = \frac{(\partial p/T^4)}{\partial(\mu/T)} : \quad \omega = \frac{\kappa_2}{\kappa_1} \ , \quad S\sigma = \frac{\kappa_3}{\kappa_2} \ , \quad \kappa\sigma^2 = \frac{\kappa_4}{\kappa_2} \tag{10}$$

Scaled Variance

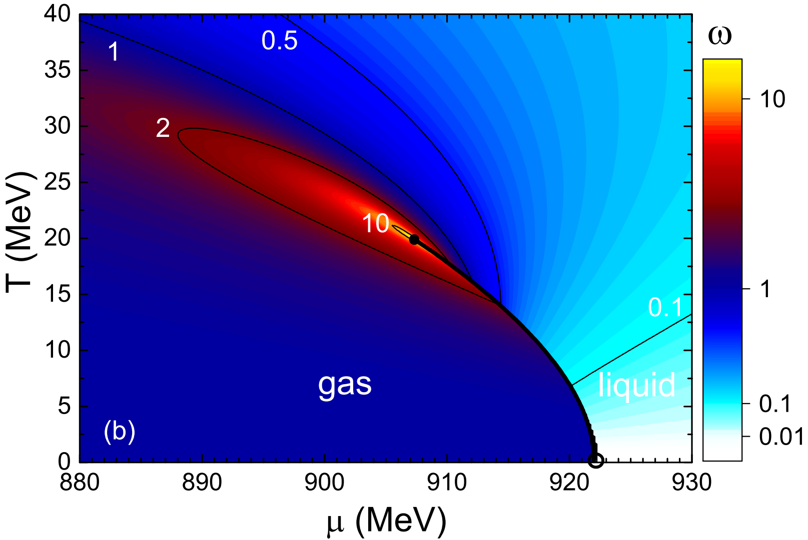

Skewness

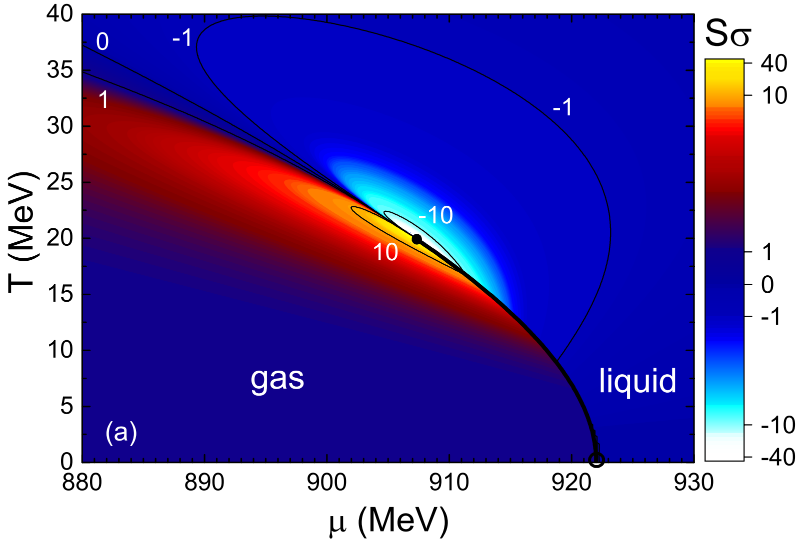
40
35
30
25
20
15
10
5
0
880
890
900
910
920
930
T (MeV)
μ (MeV)
0
-1
1
-1
-10
10
gas
liquid
(a)
Sσ
40
10
1
0
-1
-10
-40

Kurtosis

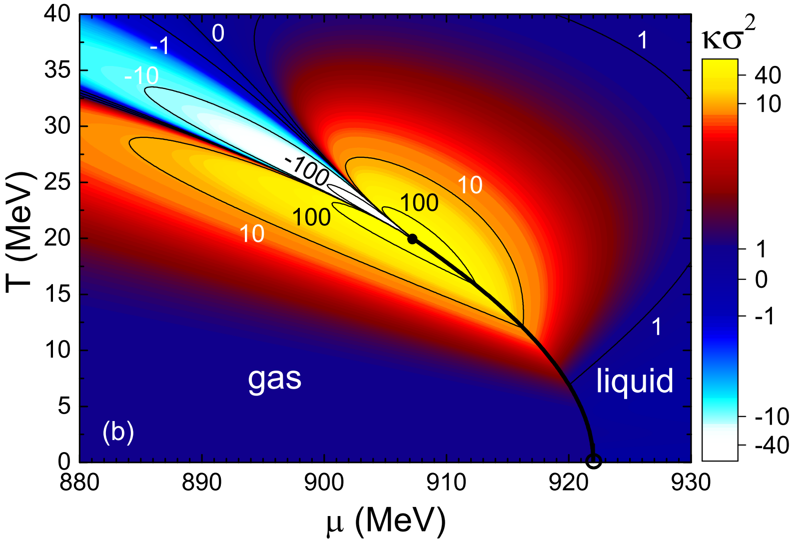
$\kappa\sigma^2$
40
10
1
0
-1
-10
-40
T (MeV)
40
35
30
25
20
15
10
5
0
880
890
900
910
920
930
μ (MeV)
-1
0
-10
-100
1
10
100
100
10
1
gas
liquid
(b)

Partition function

$$E = \sum_{j=1}^{N} \frac{\mathbf{p}_j^2}{2m} + \sum_{1 \le i < j \le N} V(|\mathbf{r}_i - \mathbf{r}_j|) \ , \tag{11}$$

$$Z(V,T,N) = \frac{1}{N!} \prod_{j=1}^{N} \int d^3 p_j \int_V \frac{d^3 r_j}{(2\pi)^3} \ \exp\left[- \frac{E}{T} \right] \tag{12}$$

$$= \frac{1}{N!} \left(\frac{mT}{2\pi} \right)^{3/2} \int_V d^3 r_1 \ldots \int_V d^3 r_N \exp\left[- \frac{1}{T} \sum_{1 \le i < j \le N} V(|r_i - r_j|) \right]$$

$$p(V,T,N) = T \left(\frac{\partial \ln Z}{\partial V} \right)_{T,N} . \tag{13}$$

Lennard-Jones pair potential

$$V_{\mathrm{LJ}}(r) = 4\varepsilon\left[\left(\frac{\sigma}{r}\right)^{12} - \left(\frac{\sigma}{r}\right)^{6}\right] , \qquad (14)$$

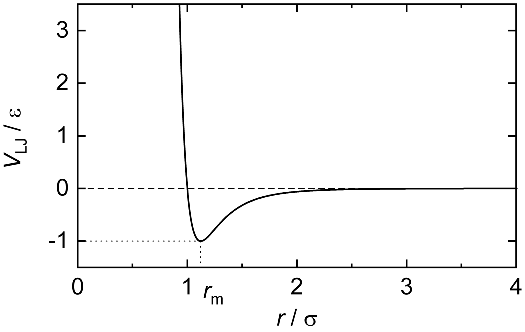

$$T_c = (1.321 \pm 0.007)\varepsilon , \quad n_c = (0.316 \pm 0.005)\sigma^{-3} . \qquad (15)$$

LJ phase diagram

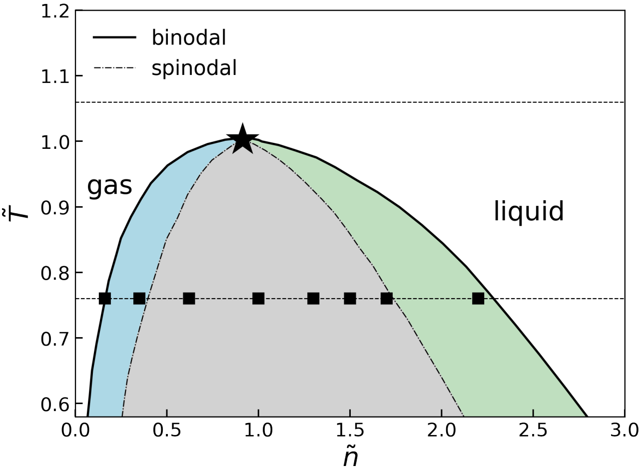

Figure: The liquid-gas region of the Lennard-Jones fluid phase diagram. Horizontal dashed lines show the subcritical isotherm $\tilde{T} = 0.76$ studied in this work and the supercritical isotherm $\tilde{T} = 1.06$.

van der Waals

$$p = \frac{nT}{1-bn} \; - \; an^2 \tag{16}$$

$$\omega \; = \; \left[\frac{1}{(1-bn)^2} \; - \; \frac{2an}{T}\right]^{-1} \tag{17}$$

$$S\sigma \; = \; \omega^2 \, \frac{1-3bn}{(1-bn)^3} \tag{18}$$

$$\kappa\sigma^2 \; = \; 3(S\sigma)^2 - 2\omega \; S\sigma - 6 \; \omega^3 \frac{(bn)^2}{(1-bn)^4} \tag{19}$$

Poberezhnyuk, Vovchenko, Anchishkin, Gorenstein, J. Phys. G (2015).
At small density $bn \ll 1$ and $an/T \ll 1$:

$$p_{\rm id} \cong Tn \; , \quad \omega_{\rm id} \cong 1 \; , \quad S\sigma_{\rm id} \cong 1 \; , \quad \kappa\sigma^2_{\rm id} \cong 1 \tag{20}$$

MD particle number fluctuations

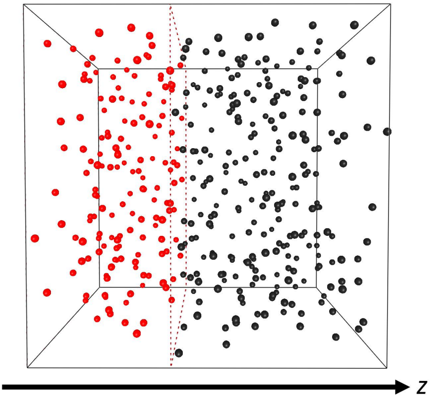

Figure: $0 < \alpha < 1$ is a fraction of the total volume occupied by the accepted particles.

Subensemble method – correction for global conservation

Cumulants, corrected for the baryon conservation reads (**V Vovchenko O. Savchuk, R. Poberezhnyuk, M. Gorenstein, V. Koch, Phys. Let. B, 2020**)

$$\tilde{\omega} \equiv \omega/(1-\alpha), \tag{21}$$

$$\widetilde{s\sigma} \equiv s\sigma/(1-2\alpha), \tag{22}$$

$$\widetilde{\kappa\sigma}^2 \equiv \frac{1}{(1-3\alpha(1-\alpha))}\kappa\sigma^2 - \frac{3\alpha(1-\alpha)}{1-3\alpha(1-\alpha)}(\widetilde{s\sigma})^2, \tag{23}$$

where $\alpha = N/N$ - subensemble fraction.

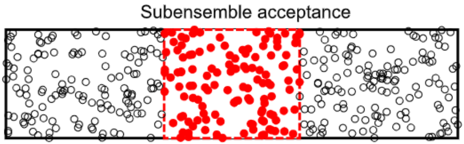

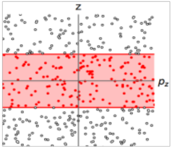

Scaled variants at $T = 1.06\ T_c$

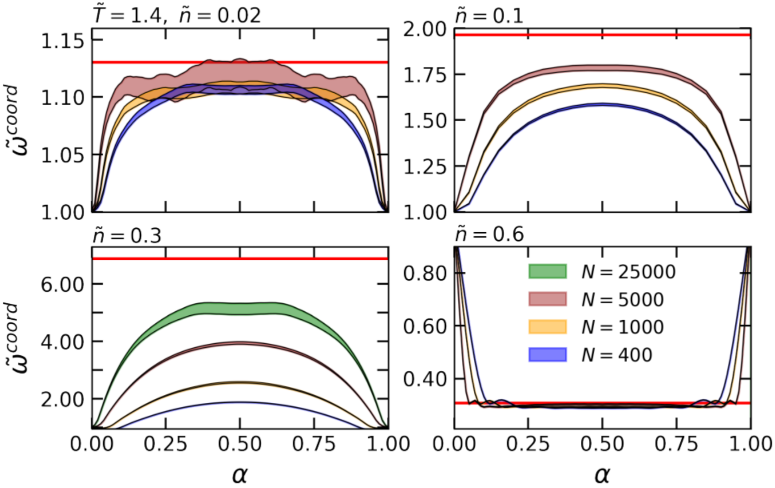

Particle number distributions at $T = 0.76\ T_c$

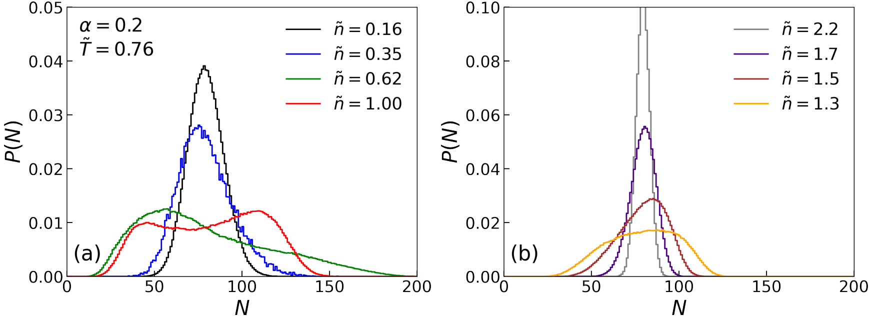

$$N_0 = 400\ , \quad n \equiv \frac{N_0}{V_0}\ , \quad V = \alpha V_0\ , \quad \alpha = 0.2\ , \tag{24}$$

$$\omega[N] \ = \ \frac{\langle N^2\rangle \ - \ \langle N\rangle^2}{\langle N\rangle}\ , \tag{25}$$

$$\langle N^k\rangle \ \equiv \ \sum_N N^k\, P(N)\ . \tag{26}$$

Molecular dynamics for ω

$T = 0.76\ T_c$ **$T = 1.06\ T_c$**

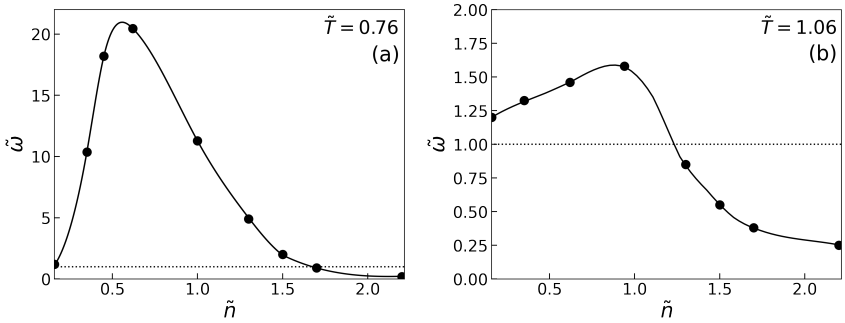

The scaled variance $\tilde{\omega}$ as a function of the particle number density $\tilde{n}$ for $\mathbf{N_0 = 400}$, $\alpha = \mathbf{0.2}$ at $\tilde{T} = 0.76$ (a) and $\tilde{T} = 1.06$ (b).

Mixed phase regions

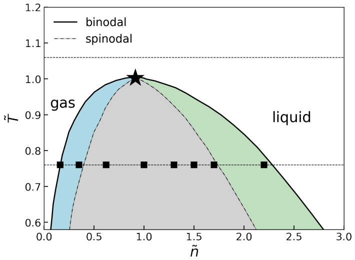

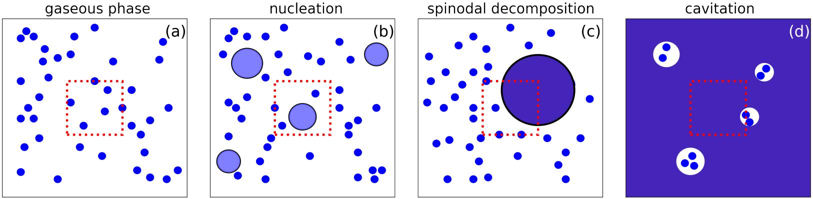

Different regions along the supercritical isotherm of the liquid-gas transition: (a) gaseous phase, (b) nucleation, (c) spinodal decomposition, and (d) cavitation.

Spinodal decomposition region

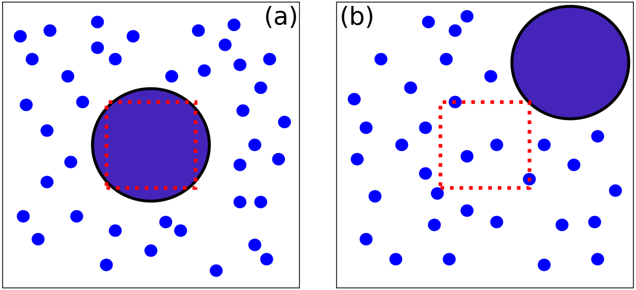

Possible position of the liquid phase in the spinodal decomposition region relative to the acceptance subvolume (red dashed square).

UrQMD simulations

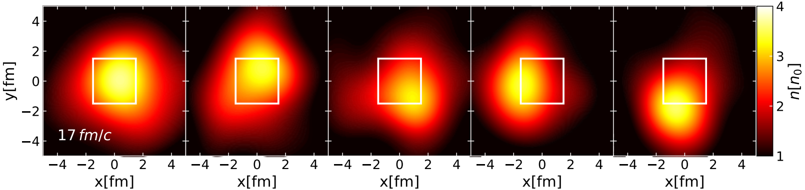

Baryon number densities in five different events in the transverse coordinate plane $z = 0$ at $t = 17$ fm$/c$ in Au+Au central collisions at $E_{\rm lab} = 2A$ GeV for the PT EoS.

O. Savchuk, R. Poberezhnyuk, A. Motornenko, J. Steinheimer, M. Gorenstein, and V. Vovchenko, Phys. Rev. C (2023)

Simple model of clusters

In the mixture of particles and k-drops one find

$$p \;=\; \frac{nT}{\langle k\rangle}\;, \tag{27}$$

$$\omega = T\left[\frac{dp}{dn}\right]^{-1} = \frac{T}{n}\left(\frac{\partial n}{\partial \mu}\right)_T = \frac{\langle k^2\rangle}{\langle k\rangle}\;, \tag{28}$$

where $\langle k^n\rangle \equiv \sum_{k\geq 1} k^n P_k$.
Due to the evident inequalities,

$$\langle k\rangle \geq 1 \quad \text{and} \quad \langle k^2\rangle \geq \langle k\rangle\;,$$

one finds

$$p \;\leq\; nT \;= p_{\rm id}\;, \quad \omega \;\geq\; 1\;\omega_{\rm id} \tag{29}$$

Higher order fluctuations, e.g., $S\sigma$ and $\kappa\sigma^2$, are expressed through $\langle k^n\rangle$.

MD at $T = 1.06\ T_c$

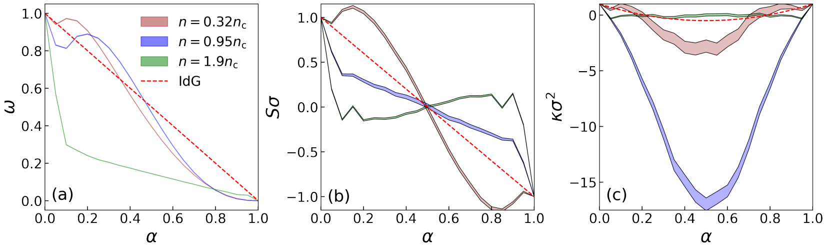
$n = 0.32 n_c$
$n = 0.95 n_c$
$n = 1.9 n_c$
IdG
(a)
(b)
(c)
ω
$S\sigma$
$\kappa\sigma^2$
α

Fluctuations with global conservation corrections

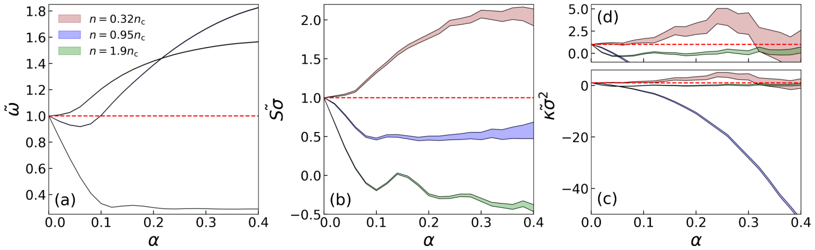

Note! Higher corrected cumulants have pole at $\alpha = 0.5$, which leads to the artificial infinities because we compute the moments values with finite precision.

Thermodynamic Limit, GCE

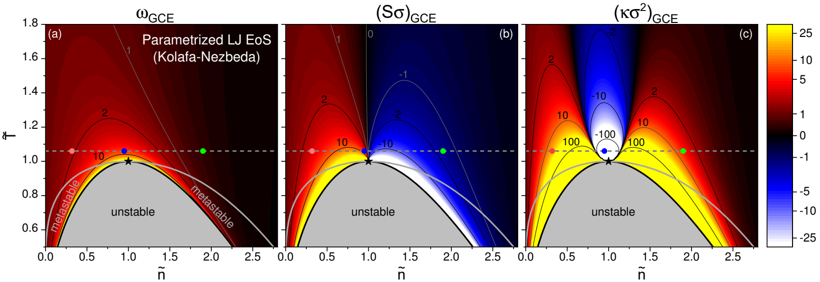

Scaled variance Skewness Kurtosis

MD calculations versus thermodynamic limit

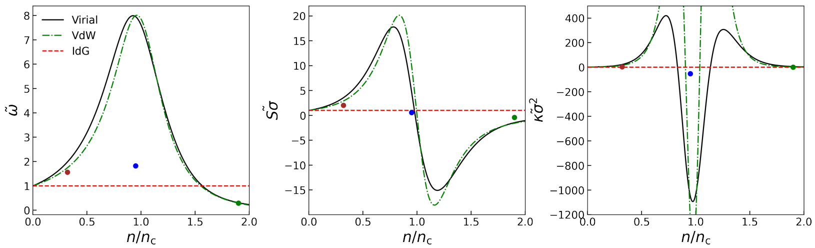

Scaled variance

Skewness

Kurtosis

Summary

MD simulations of the Lennard-Jones fluid: $N_0 = 400$ particles in a cubic box V_0. Acceptance volume is $V = \alpha V_0$.

1. At $T > T_c$ the scaled variance ω first increases with density from $\omega \approx 1$ at small n to its maximum above unity around the critical density $n = n_c$, and then it decreases with n to small values $\omega < 1$.

2. At $T < T_c$ the structure of the $P(N)$ distribution is significantly more intricate. For $n \approx n_c$, the distribution is bi-modal and $\omega \gg 1$.

3. At $T > T_c$ the kurtosis becomes strongly negative, $\kappa\sigma^2 \ll 1$, on the crossover side near the critical point.

4. The particle number fluctuations are absent in the momentum space. Strong collective flow (high collision energies) is needed to see the particle number fluctuations.